

V CIRP Conference on Biomanufacturing

# In-situ monitoring of defects in extrusion-based bioprinting processes using visible light imaging

Simone Giovanni Gugliandolo<sup>a,b</sup>, Alessandro Margarita<sup>a</sup>, Silvia Santoni<sup>a,b</sup>, Davide Moscatelli<sup>b</sup>, Bianca Maria Colosimo<sup>a\*</sup>

<sup>a</sup>Department of Mechanical Engineering, Politecnico di Milano, Via La Masa, 1, 20156, Milano, Italy

<sup>b</sup>Department of Chemistry, Materials and Chemical Engineering “Giulio Natta”, Politecnico di Milano, Piazza Leonardo da Vinci, 32, 20133, Milano, Italy

\* Corresponding author. E-mail address: [biancamaria.colosimo@polimi.it](mailto:biancamaria.colosimo@polimi.it)

## Abstract

Tissue engineering techniques are central for the development of biomedical scaffolds, which are primarily employed in the biofabrication of various artificial human tissue and organ models. Bioprinting is a new technique of creating tissue constructs that can sustain cell proliferation. The development of printing techniques proceeds together with the development of the biomaterials to be printed, which is why studying the printability of these specific biomaterials must be explored. An appropriate hydrogel used as bioink should have numerous rheological, mechanical, and biological properties for producing appropriate tissue constructs. However, reaching the right trade-off between a desirable bioactivity and high printability is challenging, and despite numerous optimization studies for different materials, printing defects often occur during printing. Herein, methods are proposed to automatically identify these drifting processes in commonly used geometries and how they affected subsequent layers, as well as printing defects within each layer. Several structures were printed with standard commercial bioink as proof of concept. The constructs were analyzed using optical images from a coaxial camera. The images were then digitally processed to get geometrical data from which patterns of defectology to be monitored were derived. This automation should decrease the time in post-processing characterization of constructs and should provide a standardized tool to compare different bioinks.

© 2022 The Authors. Published by Elsevier B.V.

This is an open access article under the CC BY-NC-ND license (<https://creativecommons.org/licenses/by-nc-nd/4.0>)

Peer-review under responsibility of the scientific committee of the V CIRP Conference on Biomanufacturing

*Keywords:* bioprinting; printability; in-situ monitoring; bioink; quality;

## Introduction

### 1 Nomenclature

AM	additive manufacturing
3D	three-dimensional
CAD	computer-aided design
SPC	statistical process control
ROI	region of interest

### State of the art

Bioprinting is an additive manufacturing (AM) technology whose goal is to fabricate parts that mimic the functionality of real tissues and organs by combining cells and biomaterials with a specific three-dimensional (3D) spatial organization. As in traditional AM, the goal is achieved with the use of computer-aided design (CAD) to generate 3D models of the geometry of the tissue or organ of interest in order to produce bioconstructs that have many applications in regenerative medicine, tissue engineering, reconstructive surgery, drug

\* Corresponding author. E-mail address: [biancamaria.colosimo@polimi.it](mailto:biancamaria.colosimo@polimi.it)

discovery, pharmacokinetics, and basic medical and cell biology research[1, 2]. Thus, one of the main challenges is to avoid the death of living cells not only during the process but also in the post-printing phases where the geometry of the printed constructs can influence the feeding possibilities of the cells.

In light of these numerous applications and due to the increasing interest in personalized medicine, bioprinting has gained the attention of both academia and industry in recent years[3]. During the last decade, many new techniques and technologies related to bioprinting have emerged in the state of the art, from specific 3D printers that fabricates bioconstructs by depositing layer-by-layer biomaterials, called bioprinters, to specific soft biomaterials loaded with living cells, called bioinks[4, 5].

As with traditional AM processes, different bioprinting techniques differ in how the biomaterial is deposited in layers. Some are based on nozzle deposition, which resolution depends mainly on the nozzle diameter (in the case of extrusion printing) or on the droplet formation mechanism (in the case of inkjet printing). Others are based on optical technologies, as laser beams to create droplet of bioinks (laser-assisted bioprinting) or light used as initiator of photopolymerization (using the traditional or two-photon process)[6–9].

The bioprinting literature is very rich with articles that address method classifications, biomaterials, and tissues investigated[5, 10], but lacks papers focused on tools and methods for measuring the quality of printed geometries, and eventually controlling and correcting deposition errors[11–13].

Nowadays, extrusion-based bioprinting is the most common and studied printing technology in the field, but, despite recent technological advances, the fabrication of good quality constructs remains a major challenge. The main limitations of extrusion bioprinted constructs are the low spatial resolution and the low accuracy in depositing materials (discontinuity, nonuniformity and irregularity[14]).

The lack of quality assurance of parts produced via bioprinting is a key technological barrier to the development of products of increasing complexity, like vascularization. Moreover, the development of non-destructive monitoring systems would allow the implementation of in-line control methods for the printing processes themselves.

Bioprinting technology is growing very fast and in the last few years the interest is increasing also in the industrial sector, from biopharmaceuticals to food[3]. While, from the biological point of view there are several vital and metabolic assays that can be used (although most of them are destructive tests), for metrological control of bioprinted constructs there is not a wide range of useful technologies implemented in both commercial and custom printers of the various research institutions studying bioprinting, even though many types of sensors have been studied as for the traditional filament fusion 3D printing[15].

Among non-destructive non-invasive methods the only one used are the image-based analysis methods with images retrieved from laser displacement scanner[11–13], cameras[14, 16, 17] or from optical coherence tomography[18–20]. Such methods are time- and cost-saving tools which are useable for

printer characterization, bioink printability evaluation and process optimization[21]. In general, these few examples of *in-situ* process monitoring systems aimed to ensure better structural and functional performances of 3D functional tissue constructs. Image processing can also be used for the study of reproducibility, since reliable production is important in the transition from research to industrial application, and more precisely to clinical studies[22].

The aim of this paper is to identify the current opportunities in the field of *ex-situ* and *in-situ* monitoring currently explored in extrusion-based bioprinting, and to try to propose possible solutions by integrating image analysis and statistical process control (SPC), not only to increase product quality but also for diagnostic analysis.

The proposed monitoring system would fit in the context of advanced manufacturing solutions, improving the digitization of processes and systems, the management of "Big Data" and the fusion/integration of information from multiple sensors. It would also open the opportunity in developing a process control system, to modify control inputs to correct errors in subsequent layers[23]. This would be a key contribution to defining a new method to quantitatively evaluate the accuracy of printed constructs and improve their quality.

The paper is structured as follows: in section 2 the materials and method used are described. In section 3, preliminary results of such an approach are herein presented. In section 4 critical issues and advantages of this approach are discussed. Finally, the main conclusions are drawn in section 5.

## Materials and Methods

### Experimental Setup

For this study we used a pneumatic extrusion-based bioprinter, the BIO X (CELLINK, Gothenburg, Sweden).

A square lattice pattern (15x15 mm in size in x-y plane and with a height of 4 mm, 20% infill density), commonly used in the bioprinting field, was chosen as printing sample.

As testing material, we have used a commercial sodium alginate-based material, the CELLINK XPLORE (CELLINK, Gothenburg, Sweden). The ink is non-sterile and specifically designed for prototypes and tests, but its rheological and chemical properties are similar to CELLINK BIOINK, that is commonly used as material for experiments with cells. This leads to the possibility to consider the results of the experiments reproducible also with sterile and more cell-friendly bioinks of the same type and chemical composition.

A 3 ml cartridge was filled with the above-mentioned ink, and it was loaded on the extrusion head of the BIO X printer. A printing nozzle with an inner diameter of 22 G (0.41 mm) was attached to the cartridge; this led to print constructs of 10 layers.

Once nozzle size and material were defined, the two main process parameters, pressure and print speed, were modified accordingly to manufacturer indications to obtain the best printability of the selected bioink. Pressure was set at 22kPa

and print speed at 10mm/s. Ideally, these parameters should have guaranteed a defect-free printing of the construct.

A set of five constructs were printed. In two constructs, over extrusion defects were caused by manually increasing dispensing pressure in some higher layer, to simulate and emphasize what might happen because of rheological changes within a bioink, usually caused by uncontrolled changes in process parameters (temperature changes, presence of bubbles, etc.). Temperature was set to 37°C, both at the printhead and at the printbed, to mimic experimental condition suitable for cells.

### Process sensing

The images were taken using the integrated high-definition (1280x720) camera present on the bioprinter; the camera was mounted close to the printhead, letting us acquire *in-situ* co-axial images. A black background has been placed on the printbed to increase the contrast and reduce reflectivity phenomena, for a better acquisition of images. The images were then processed by a custom-made MATLAB® R2020b (MathWorks, Natick, USA) script. Only one manual calibration of the machine (for both axis movement and camera focusing) was performed before the entire printing session.

The integrated HD camera automatically moves over the construct after each layer is printed and takes pictures of the sample (Figure 1). The images are saved to mobile storage device and are then processed with a computer.

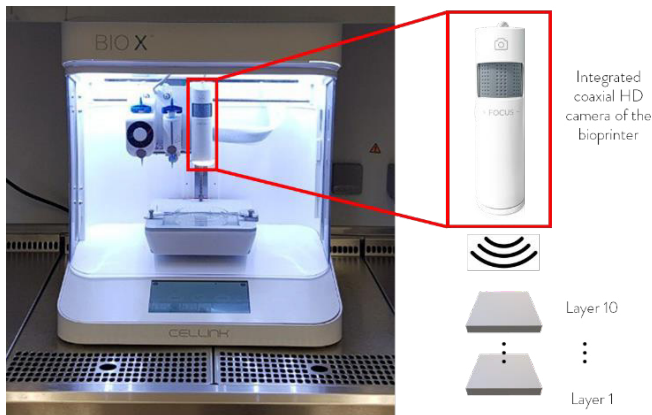


Figure 1. Experimental set-up. The integrated HD camera of the bioprinter automatically moves over the construct after each layer is printed and captures the photo.

### Image and statistical analysis

The proposed method started after data gathering and data preparation for image processing and then resulted in the statistical analysis of the acquired data.

Image processing was the first core stage and was currently based on custom-made methods of image registration, segmentation and binarization. The algorithm was applied to images of the bioprinted sample, taken after the printing of each layer. In points:

- in the first step the image of a layer was cropped and rotated around the region of interest. This was done to reduce the size of the images to which the next steps are to be applied, to reduce the workload and processing time. Landmark points were placed on it for further registration operations.
- in the second step the image was segmented through the K-means clustering function of MATLAB®, *imsegkmeans*, that is one of the most popular iterative algorithms in clustering and segmentation. The K-means algorithm was used to partition an image into  $k$  clusters. The  $k$  cluster were manually selected to identify foreground, background and region of interest (ROI) excluded background. This led to the choice of  $k = 4$  and  $k = 3$  depending on whether there were artificially introduced errors or not, respectively. The algorithm assigns each pixel in the image to the cluster that minimizes the distance between the pixel and the cluster center, based on the color of each pixel. Then re-computes the cluster centers by averaging all of the pixels in the cluster and repeats the previous two steps until convergence is attained (i.e. no pixels change clusters) [24].
- in the third step a binary image containing only the pixel of the pre-processed ROI was obtained, where pixels with value 1 indicated pixels where the material was present and 0 where there was void.

As the limitations of the method were also investigated, and the first two processes were critical steps.

The binarized nominal image (where pixels with value 1 and 0 have the meaning previously stated) of the respective layer was taken from the sliced model and registered on the binarized image obtained from the camera thanks to the previously placed landmark points. The registration was performed using the *fitgeotrans* function of MATLAB®, by applying the 'nonreflectivesimilarity' properties, in which, while shapes in the moving image were unchanged, the image was distorted by combination of translation, rotation, and scaling (straight lines remain straight, and parallel lines are still parallel).

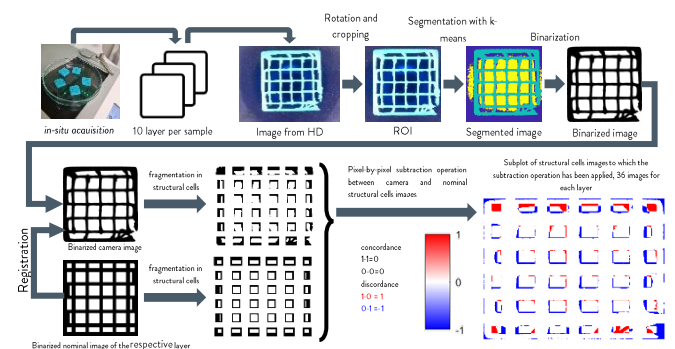


Figure 2. Example of the data and image processing of a photo of a layer. In the first step the image is rotated and cropped. In the second step it is segmented. In the third step it is binarized. Once binarized it is fragmented into the 36 structural cells and each cell is subtracted from the corresponding structural cell extracted from the binarized nominal image of the corresponding layer. The new image is formed only by pixels that have value -1, 0 and 1.

At this point the binarized nominal image of the respective layer was automatically fragmented in structural cells, through a custom-made ROI identification algorithm. In this case, due to the type of infill pattern (and the relative infill density), the structure was formed by 36 structural cells, some of which of flatter dimensions near the perimeter of the construct (see the nominal image of a layer in Figure 2).

Thanks to the previous registration, these structural cells were superimposed on the binarized image obtained by the integrated camera to get the respective structural cell that have to be monitored layer-by-layer.

Then the algorithm automatically performed a pixel-by-pixel subtraction operation between the binarized cell of the nominal image of the respective layer and the binarized structural cell of the camera image (Figure 2).

Thus, the new binarized image of the structural cell was a matrix in which only three results were possible: 0 where there was correspondence (void where should be void, 0-0=0; and material where should be material, 1-1=0) and 1 or -1 where there is discrepancy (over extrusion, where there is material where should be void, 1-0=1; and under extrusion, where vice versa, 0-1= -1). A subplot of 36 images per layer, as shown in the bottom-right image of Figure 2, was obtained for each layer.

A normalized metric called *Over Extrusion* was calculated for the over extrusion defect outcome. It was defined as the sum of all the pixel with value 1 with respect to the area of the structural cell under consideration, as this could change depending on whether the structural cell is at the edges or in the center of the construct (details of a structural cell analysis in Figure 3):

$$Over\ Extrusion = \frac{\sum pixel\ with\ value\ 1}{Area\ unit}$$

The values were then used to produce an interval plot to assess and compare the 95% confidence intervals of the means of each group.

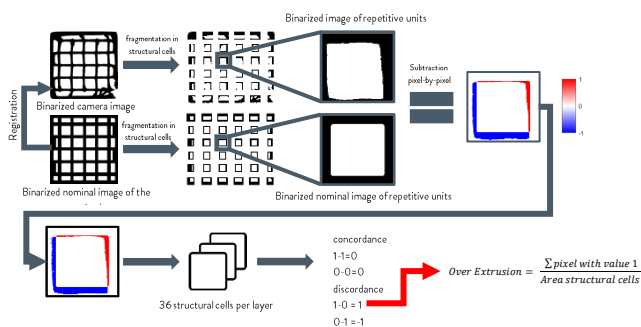


Figure 3. Detail of the analysis of a single structural cell. After pixel-by-pixel subtraction all pixels with value 1 are summed to obtain the *Over Extrusion* metric.

## Results

### Printing results

Although all 5 samples were successfully printed up to the 10<sup>th</sup> layer, almost all of them showed major and minor errors, especially in higher layers. From a visual inspection the inner voids of the grids were well defined and presented only minor defects, while the voids closer to the perimeter of the grids did not present the nominal squared shape. Moreover, during the printing phase it was possible to notice that from the sixth layer the weight of the layers below and the shrinkage of the already deposited material caused a compression of the construct, resulting in defects in the printing process due to the small gap between the underlying layers and the nozzle.

In Table 1 the results of visual inspection are reported, to be compared with the results obtained in the following paragraph.

Condition	Sample	Layer									
		1	2	3	4	5	6	7	8	9	10
P = 22 kPa V = 10 mm/s	1	Green	Green	Green	Green	Green	Red	Red	Red	Red	Red
	2	Green	Green	Green	Green	Green	Red	Red	Red	Red	Red
	3	Green	Green	Green	Green	Green	Red	Red	Red	Red	Red
	4	Green	Green	Green	Green	Green	Blue	Blue	Red	Red	Red
	5	Green	Green	Green	Green	Green	Blue	Blue	Red	Red	Red

Table 1. Results of visual inspection: green boxes show layers with minor or no defects; blue boxes show layers where errors were manually added; red boxes show layers with major defects.

### 1.1. Image and statistical results

A complete dataset of 50 images has been obtained and analyzed. Visual interpretation of all the obtained segmented and binarized images (example in Figure 2) confirmed the suitability of the chosen value for *k*.

Each image was automatically divided into 36 cells. For each cell, a value of *Over Extrusion* was obtained. Interval plots with 95% confidence intervals of the means of the 36 values of each layer are shown in Figure 4. The *Over Extrusion* metric showed an increasing trend as the layers increase in all the samples, even if with different slopes. It is possible to see that, although samples 1, 2 and 3 were “in control”, a slight drifting process in subsequent layers took place up to an *Over Extrusion* of 10%. Regarding sample 4 and 5 the introduction of major defects of over extrusion are clearly visible after layer 7, with *Over Extrusion* value above 20%.

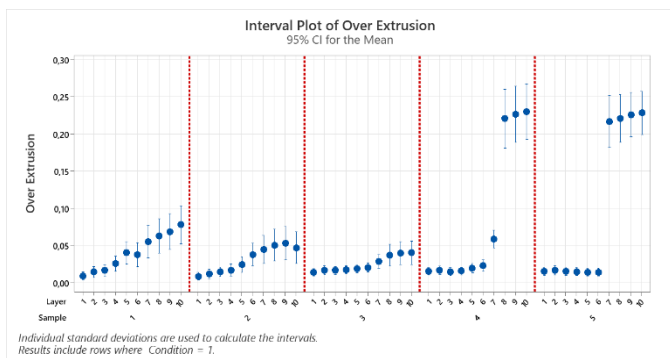


Figure 4. Interval plots with 95% confidence intervals of the means of the metric *Over Extrusion*, for each layer of each sample.

#### 4. Discussion

Accuracy in bioprinting process is currently limited by the lack of error monitoring techniques. Although the identification and the study of relationships between printing outcomes and process parameters were widely investigated, repeatability of the printing process is still far from being reached, especially in extrusion-based bioprinting[25]. Strauß, S. et al. used in their work non-invasive image-based analysis methods as tool for line construct characterization. It was an automated method to enable comparison of 3D printed lines to evaluate the influence of rheological properties and printing parameters on them[16]. Armstrong et al. used point cloud data from a laser scanner to obtain images of the printed samples. They then use a custom image processing algorithm to determine the error between the reference and printed trajectory[11–13]. A different approach was used by Wang, L. et al. In this study, optical coherence tomography was applied to acquire high-resolution images of hydrogel scaffolds. An image analysis algorithm was proposed to accurately quantify some morphological parameters (pore size, pore shape, surface area, porosity, and interconnectivity) and to develop a method for non-destructive and quantitative geometric characterization of printed scaffolds[18–20].

Monitoring may become a key factor for the spread of bioprinting technologies, in a context where more complex applications are needed. Through our study we have showed that it is possible to develop a layer-by-layer monitoring algorithm able to detect printing defects suitable for usage with cells.

The method used in our work identified drift phenomena during the printing process. These were certainly more evident where the artificially added errors were introduced, with values of *Over Extrusion* above 20%. These errors could simulate rheological changes within bioinks, usually caused by uncontrolled changes in process parameters (temperature changes, presence of bubbles, etc.). Drifting processes were also detected in “in-control” samples, where, as expected, increasing the layers perpetuated the pre-existing condition of excessively extruded material. In both cases we were able to build a map of defects. The work here presented describe a simple monitoring experiment in which the feasibility of using visible imaging for geometry detection of printed constructs

was demonstrated. More specifically, we have demonstrated the effectiveness in being able to discriminate defect between layers. The automated monitoring system has proven to be able to detect defects in deposition, giving to the operator a full understanding of the moment and the layer where the defect occurred, enabling the adoption of countermeasures in subsequent prints.

Despite the encouraging results of the method used there are still several limitations that need to be addressed. The presented method suffers the common limitations of systems and devices operating with visible light (such as cameras) since they would be affected by the ambient brightness and transparency conditions of the bioinks. In some cases, the sensing system might be minimally affected by light reflected on the bioprinted construct, this would require the development of even more robust algorithms. Moreover, an image acquisition device with higher resolution and an integrated lighting system might solve such issues, increasing the reproducibility and the precision of measurements.

Furthermore, in this study it should also be taken into account that, although the printing temperature was kept constant during the printing process, there was no possibility to control the temperature of the extrusion nozzle, due to the temperature control system of the bioprinter; this may have caused a slight change in the rheology of the ink due to the possible modifications of the ambient temperature, resulting in small differences in printing resolution.

Moreover, the structure of the upper layers of the constructs was affected by the weight of the underlying layers and the shrinkage of the already deposited material, causing the not perfect deposition of ink and a lower printing resolution.

Finally, it has to be said that the analysis of cells in which images were divided was not performed in real time.

Despite these limitations this approach would also open the opportunity in developing a process control system, able to modify control inputs and to correct errors in subsequent layers. This approach may be of interest not only for the end-users of extrusion bioprinters but also for manufacturers of bioprinters, since a monitoring system like the one proposed can be implemented also in machines already present on the market or added as a compatible tool for new bioprinters.

As future development, a better image processing system, capable to identify more features and able to operate in real-time should be developed. *In-situ* monitoring techniques with application of feedback systems for process control should also be implemented.

The objective of this work is to take a first step in this direction. The results obtained have shown that it is possible to use this technique for the identification of defects, thus opening the doors to the development of new lines of research concerning the in-line monitoring for this type of processes.

#### 4. Conclusions

3D bioprinting has a great potential for future expansions. In recent years, the growing interest from universities and

companies has shifted attention to the critical issues that still need to be addressed to improve these technologies.

In the perspective of a shift towards production requirements, the need to develop techniques for quality control monitoring becomes increasingly evident.

This work has demonstrated that there is workspace for the implementation of *in-situ* monitoring methods for bioprinting processes, despite the technological limitations and simplicity of the proof of concept described.

We plan to develop alert systems able to identify several parameters at a time, geometric and non-geometric, detected by multiple types of sensors to realize a real *in-situ* monitoring platform, possibly based on machine learning and data fusion approaches following the path of process digitalization.

### Acknowledgements

This research has been partially funded by Agenzia Spaziale Italiana -ASI under the joint project PoliMi-ASI.

### References

- Moroni L, Boland T, Burdick JA, et al., Biofabrication: A Guide to Technology and Terminology, (2018)
- Ng WL, Chua CK, Shen YF, (2019) Print Me An Organ! Why We Are Not There Yet. *Prog. Polym. Sci.* 97 : 101145. <https://doi.org/10.1016/j.progpolymsci.2019.101145>
- Santoni S, Gugliandolo SG, Sponchioni M, et al., (2021) 3D bioprinting: current status and trends—a guide to the literature and industrial practice. *Bio-Design Manuf.* 2021 51. 5 (1) : 14–42. <https://doi.org/10.1007/S42242-021-00165-0>
- Pereira FDAS, Parfenov V, Khesuani YD, et al., (2018) Commercial 3D Bioprinters. *3D Print. Biofabrication.* : 535–549. [https://doi.org/10.1007/978-3-319-45444-3\\_12](https://doi.org/10.1007/978-3-319-45444-3_12)
- Jang J, Park JY, Gao G, et al., Biomaterials-based 3D cell printing for next-generation therapeutics and diagnostics, (2018)
- Lee JM, Sing SL, Zhou M, et al., (2018) 3D bioprinting processes: A perspective on classification and terminology. *Int. J. Bioprinting.* 4 (2). <https://doi.org/10.18063/IJB.v4i2.151>
- Gao G, Kim BS, Jang J, et al., (2019) Recent Strategies in Extrusion-Based Three-Dimensional Cell Printing toward Organ Biofabrication. *ACS Biomater. Sci. Eng.* 5 (3) : 1150–1169. <https://doi.org/10.1021/acsbiomaterials.8b00691>
- Antoshin AA, Churbanov SN, Minaev N V., et al., (2019) LIFT-bioprinting, is it worth it? *Bioprinting.* 15 (May) : e00052. <https://doi.org/10.1016/j.bprint.2019.e00052>
- Kumar H, Kim K, Stereolithography 3D Bioprinting. In: *Methods in Molecular Biology.* pp. 93–108. Humana Press Inc. (2020)
- Sheth R, Balesh ER, Zhang YS, et al., Three-Dimensional Printing: An Enabling Technology for IR, (2016)
- Armstrong AA, Norato J, Alleyne AG, et al., (2020) Direct process feedback in extrusion-based 3D bioprinting. *Biofabrication.* 12 (1). <https://doi.org/10.1088/1758-5090/ab4d97>
- Armstrong AA, Alleyne AG, Wagoner Johnson AJ, (2020) 1D and 2D error assessment and correction for extrusion-based bioprinting using process sensing and control strategies. *Biofabrication.* 12 (4) : 045023. <https://doi.org/10.1088/1758-5090/aba8ee>
- Armstrong AA, Pfeil A, Alleyne AG, et al., (2021) Process monitoring and control strategies in extrusion-based bioprinting to fabricate spatially graded structures. *Bioprinting.* 21 (September 2020) : e00126. <https://doi.org/10.1016/j.bprint.2020.e00126>
- Jin Z, Zhang Z, Shao X, et al., (2021) Monitoring Anomalies in 3D Bioprinting with Deep Neural Networks. *ACS Biomater. Sci. Eng.* <https://doi.org/10.1021/ACSBIOMATERIALS.0C01761>
- Oleff A, Küster B, Stonis M, et al., (2021) Process monitoring for material extrusion additive manufacturing: a state-of-the-art review. *Prog. Addit. Manuf.* 2021 64. 6 (4) : 705–730. <https://doi.org/10.1007/S40964-021-00192-4>
- Strauß S, Meutelet R, Radosevic L, et al., (2021) Image analysis as PAT-Tool for use in extrusion-based bioprinting. *Bioprinting.* 21 : e00112. <https://doi.org/10.1016/J.BPRINT.2020.E00112>
- Uzun-Per M, Gillispie GJ, Tavolara TE, et al., (2021) Automated Image Analysis Methodologies to Compute Bioink Printability. *Adv. Eng. Mater.* 23 (4) : 2000900. <https://doi.org/10.1002/ADEM.202000900>
- Yang S, Wang L, Chen Q, et al., (2021) In situ process monitoring and automated multi-parameter evaluation using optical coherence tomography during extrusion-based bioprinting. *Addit. Manuf.* 47 : 102251. <https://doi.org/10.1016/J.ADDMA.2021.102251>
- Wang L, Xu ME, Luo L, et al., (2018) Iterative feedback bioprinting-derived cell-laden hydrogel scaffolds with optimal geometrical fidelity and cellular controllability. *Sci. Rep.* 8 (1) : 1–13. <https://doi.org/10.1038/s41598-018-21274-4>
- Wang L, Xu M, Zhang L, et al., (2016) Automated quantitative assessment of three-dimensional bioprinted hydrogel scaffolds using optical coherence tomography. *Biomed. Opt. Express.* 7 (3) : 894. <https://doi.org/10.1364/boe.7.000894>
- Bom S, Ribeiro R, Ribeiro HM, et al., (2022) On the progress of hydrogel-based 3D printing: Correlating rheological properties with printing behaviour. *Int. J. Pharm.* 615 : 121506. <https://doi.org/10.1016/J.IJPHARM.2022.121506>
- Yan WC, Davoodi P, Vijayavenkataraman S, et al., 3D bioprinting of skin tissue: From pre-processing to final product evaluation, (2018)
- Najjartabar Bisheh M, Chang SI, Lei S, (2021) A layer-by-layer quality monitoring framework for 3D printing. *Comput. Ind. Eng.* 157 : 107314. <https://doi.org/10.1016/J.CIE.2021.107314>
- Arthur, David and Vassilvitskii S, k-means++: The Advantages of Careful Seeding. *Proc. Annu. ACM-SIAM Symp. Discret. Algorithms.* 07 (3) : 1027–1035
- Gao T, Gillispie GJ, Copus JS, et al., (2018) Optimization of gelatin-alginate composite bioink printability using rheological parameters: A systematic approach. *Biofabrication.* 10 (3). <https://doi.org/10.1088/1758-5090/aacdc7>